Electronic Supplementary Information for

Luminescence Behaviour in Acetonitrile and in the Solid State of a Series of Lanthanide Complexes with a Single Helical Ligand

Miki Hasegawa,*[a] Hideki Ohtsu,[a,b] Daisuke Kodama,[a] Takeshi Kasai,[a]
Shoya Sakurai,[a] Ayumi Ishii,[a] and Kengo Suzuki[c]

[a] Collage of Science and Engineering, Aoyama Gakuin University 5-10-1 Fuchinobe, Chuo-ku, Sagamihara, Kanagawa 252-5259, Japan, E-mail: hasemiki@chem.aoyama.ac.jp;
[b] Graduate School of Science and Engineering, University of Toyama, 3190 Gofuku, Toyama, Toyama 930-8555, Japan;
[c] Hamamatsu Photonics K. K., 812 Joko-cho, Higashi-ku, Hamamatsu, Shizuoka 341-3196, Japan

Contents

1. Syntheses of the ligand and lanthanide complexes.

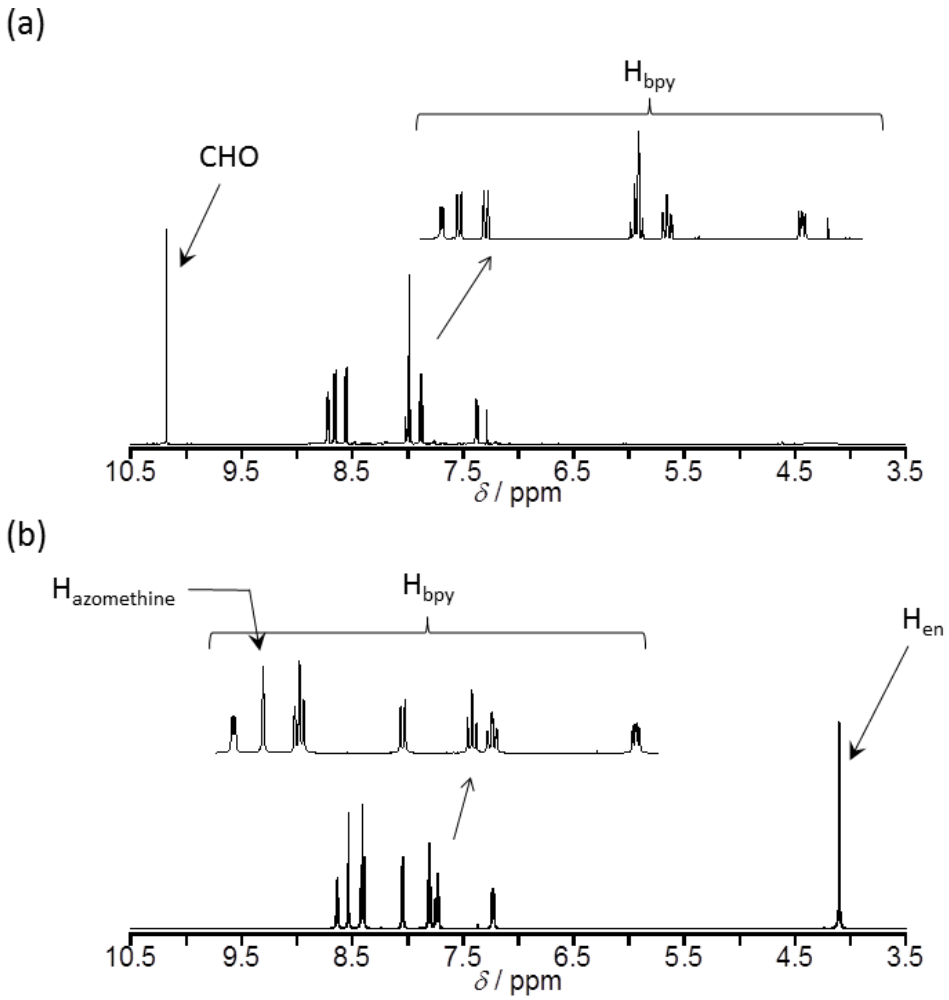

Fig. S1 ^{1}H NMR spectra of (a) bipyridine-6-aldehyde and (b) **L** in $CDCl_3$ (TMS) recorded on JMN-ECP500 (JEOL).

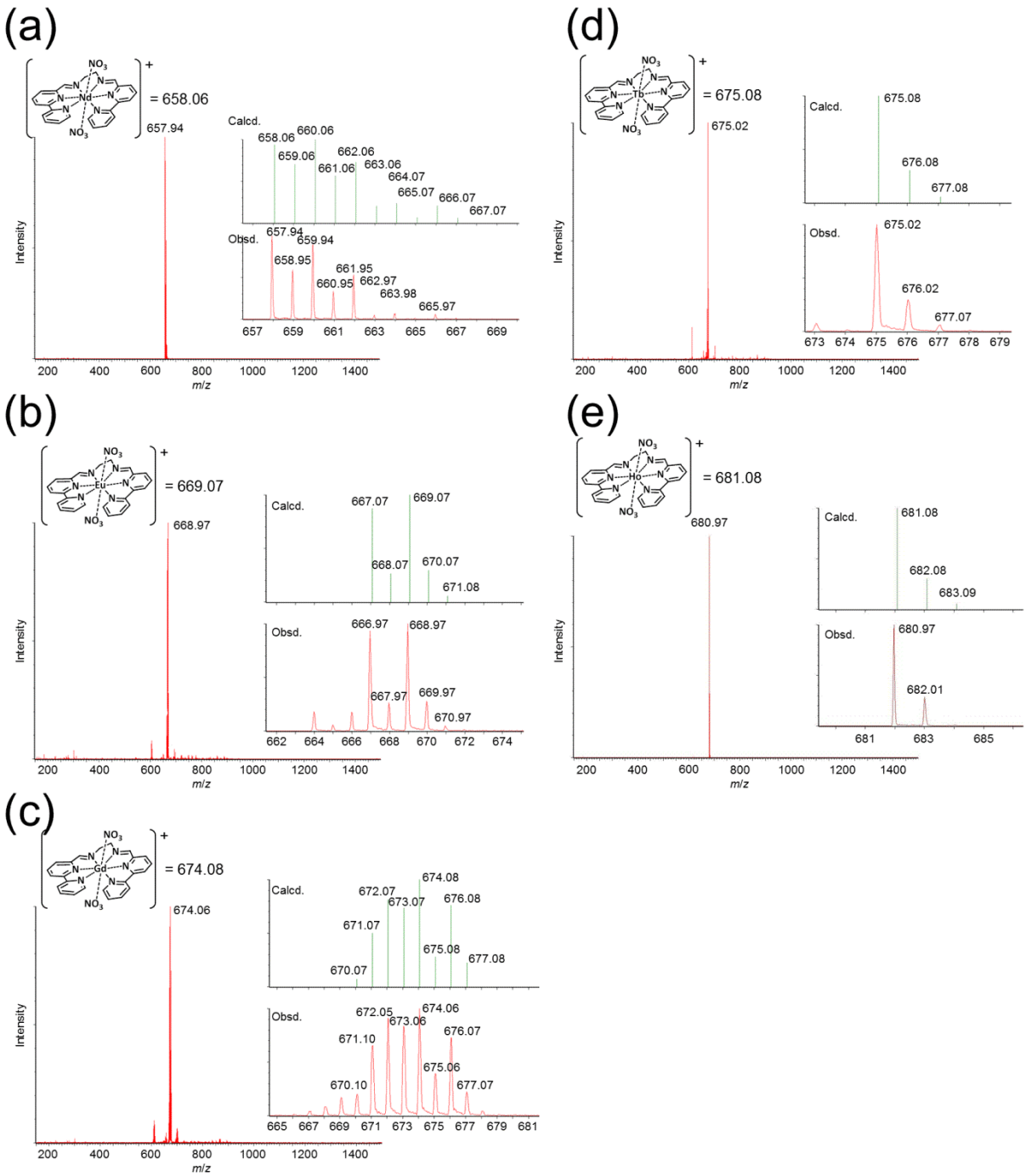

Fig. S2 ESI-TOF-MS spectra (positive mode) of (a) Nd**L**, (b) Eu**L**, (c) Gd**L**, (d) Tb**L** and (e) Ho**L** in acetonitrile. Insets show the magnified view for theoretical isotope (top) and the observed (bottom) patterns for the main peaks.

2. Crystalline data for LnL (Ln = Nd, Eu, Gd, Tb and Ho).

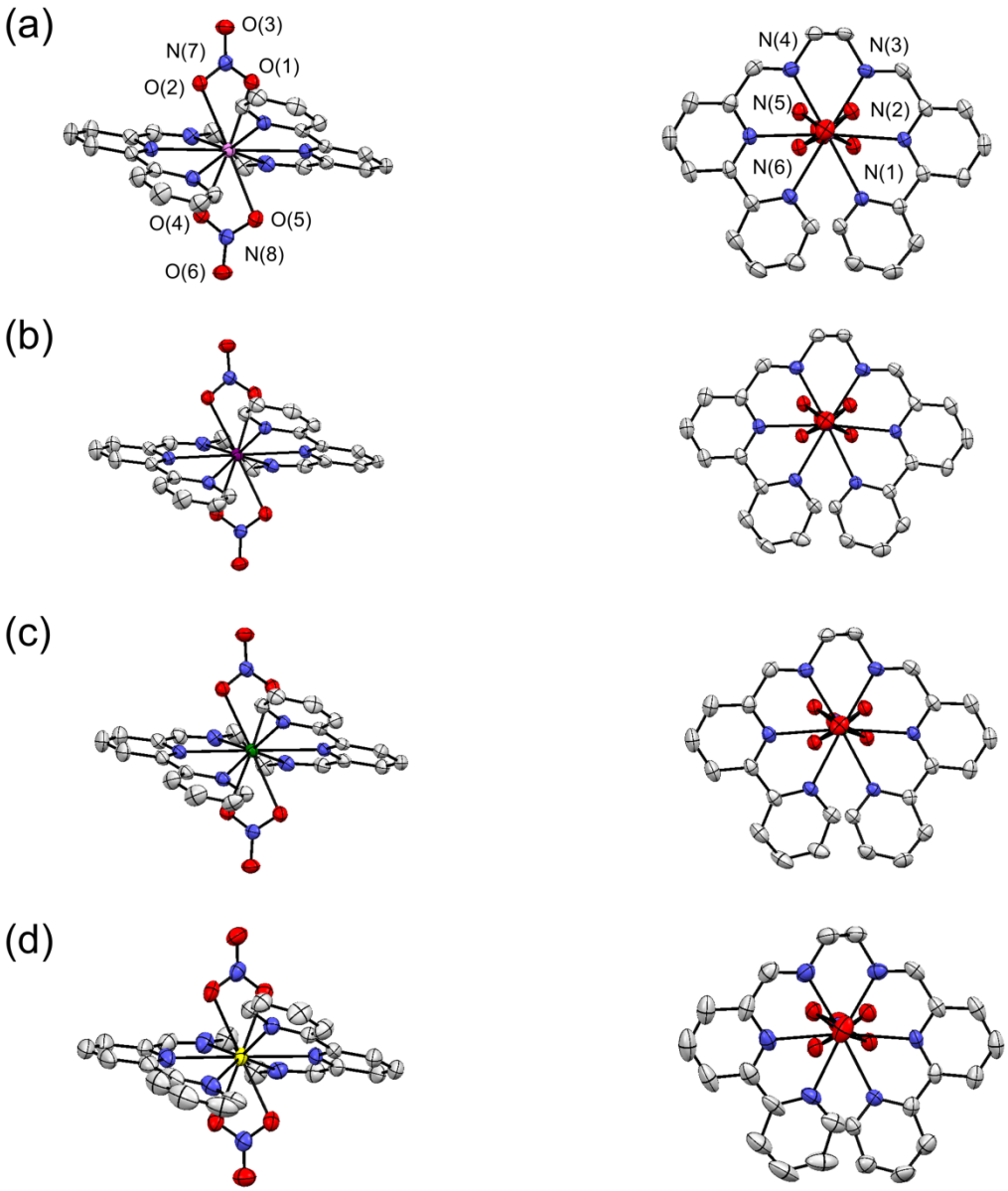

Fig. S3 ORTEP drawing of (a) Nd**L**, (b) Gd**L**, (c) Tb**L** and (d) Ho**L** with 70 % probability thermal ellipsoids. Hydrogen atoms are omitted for clarity. Gray: carbon, blue: nitrogen, Please replace this sentence to "CCDC 919427 for Eu**L**, 919428 for Gd**L**, 919429 for Ho**L**, 919430 for Nd**L** and 919431 for Tb**L**"

red: oxigen, lilac: neodimium, violet: gadrinium, green: terbium and yellow: hormium.

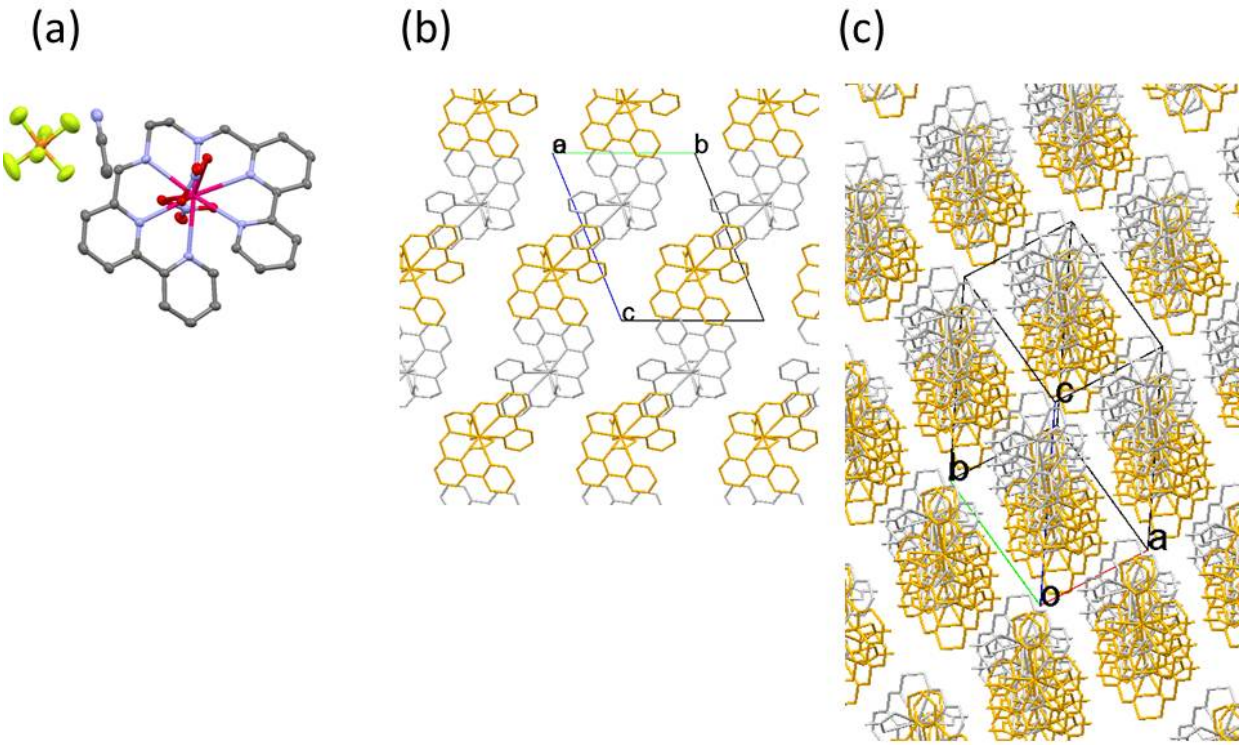

Fig. S4 (a) Molecular structure of Eu**L** with PF_6^- ion and acetonitrile. Gray: carbon, blue: nitrogen, red: oxygen, pink: europium, pale yellow: fluorine and orange: phosphorous. Molecular packing of Eu**L** projected from along the *a*-axis (b), and the crest of *b*-axis (c). Gold and silver mean left- and right-handed isomers, respectively. Hydrogen atoms, PF_6 and acetonitrile are omitted for clarity.

Table S1 Selected bond lengths and bond angles for Ln**L**.

	Nd	Eu	Gd	Tb	Ho
Ln-N(1)	2.643(3) Å	2.620(4)	2.616(4)	2.596(3)	2.576(4)
Ln-N(2)	2.645(3)	2.590(4)	2.588(4)	2.586(4)	2.538(4)
Ln-N(3)	2.572(3)	2.533(3)	2.525(3)	2.505(4)	2.487(4)
Ln-N(4)	2.570(3)	2.531(4)	2.518(4)	2.510(3)	2.490(4)
Ln-N(5)	2.629(3)	2.607(4)	2.602(4)	2.569(3)	2.543(2)
Ln-N(6)	2.652(3)	2.616(3)	2.610(3)	2.601(3)	2.615(3)
Ln-O(1)	2.546(3)	2.530(2)	2.512(2)	2.474(3)	2.469(3)
Ln-O(2)	2.541(3)	2.488(3)	2.475(3)	2.500(3)	2.460(3)
Ln-O(4)	2.570(2)	2.504(3)	2.490(3)	2.466(3)	2.472(4)
Ln-O(5)	2.522(3)	2.519(3)	2.505(3)	2.494(2)	2.453(3)
N(1)-Ln-N(2)	60.6(1)	61.5(1)	61.5(1)	61.6(1)	62.5(1)
N(2)-Ln-N(3)	62.3(1)	63.3(1)	63.4(1)	63.3(1)	64.5(1)
N(3)-Ln-N(4)	64.2(1)	64.7(1)	64.8(1)	65.0(1)	64.7(1)
N(4)-Ln-N(5)	62.63(9)	63.0(1)	63.1(1)	63.7(1)	64.4(1)
N(5)-Ln-N(6)	60.82(8)	61.2(1)	61.4(1)	61.68(9)	62.0(5)
O(1)-Ln-O(2)	50.47(8)	51.2(1)	51.36(9)	51.60(9)	52.0(9)
O(4)-Ln-O(5)	50.39(8)	51.2(1)	51.40(9)	51.71(9)	51.6(1)

Table S2 Selected mean interatomic distances and angles between skeletons for Ln**L**.

	Nd	Eu	Gd	Tb	Ho
mean Ln-N_{py} (Å)	2.642(6)	2.612(0)	2.604(3)	2.588(3)	2.568(1)
mean Ln-N_{en} (Å)	2.571(3)	2.532(4)	2.521(9)	2.507(8)	2.488(9)
mean Ln-O (Å)	2.545(0)	2.510(5)	2.495(8)	2.483(7)	2.463(8)
C(1)-C(24) (Å)	3.174(4)	3.178(6)	3.186(5)	3.198(5)	3.146(8)
$\theta_{NO_3-NO_3}$ (deg)	66.91	65.97	65.84	64.52	62.45
$\theta_{bpy\text{-}bpy}$ (deg)	31.95	31.97	32.36	32.84	28.04

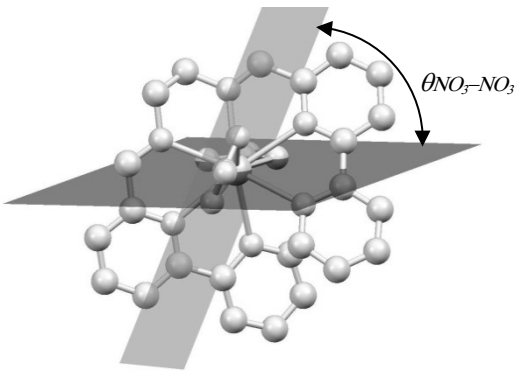

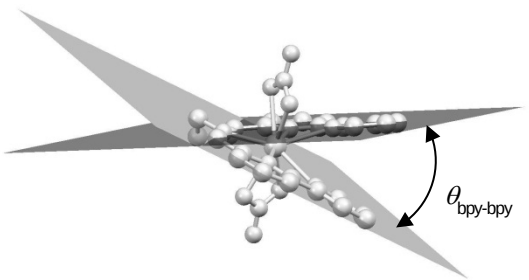

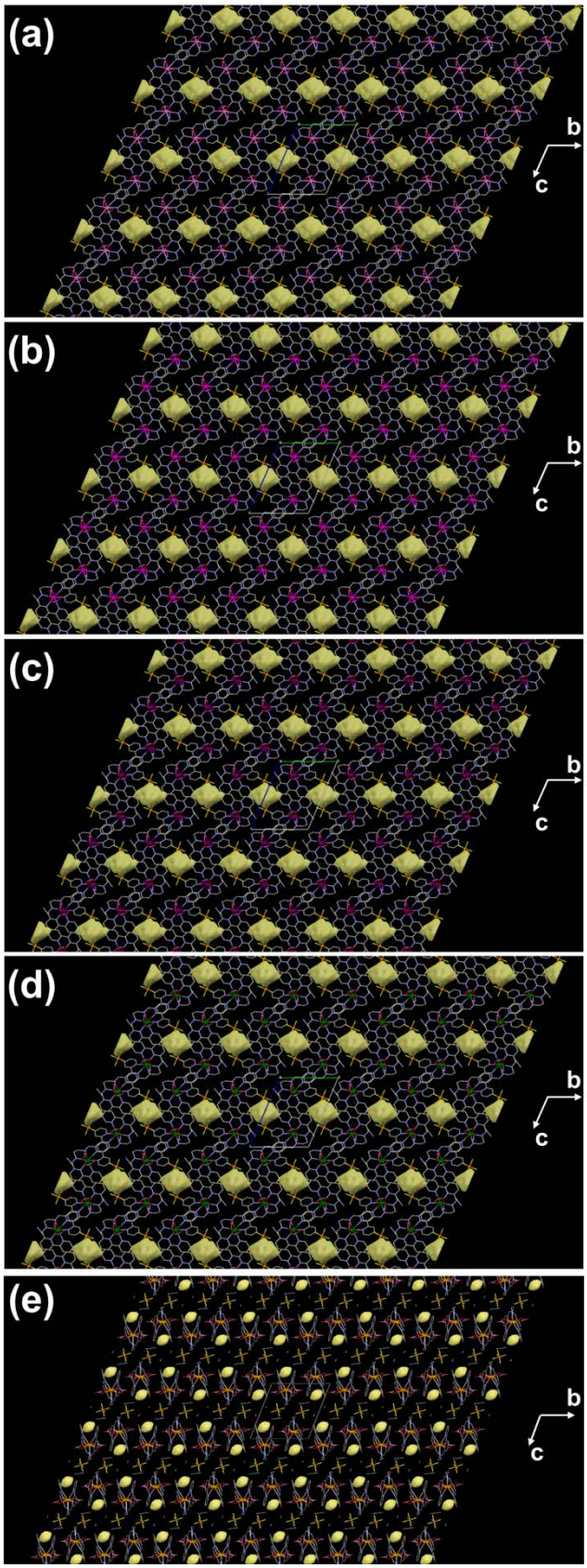

Fig. S5 Void spaces of (a) Nd**L**, (b) Eu**L**, (c) Gd**L**, (d) Tb**L** and (e) Ho**L** projected from the b-c plane.

Table S3 Pore volumes (Å ^{3}) for a series of helical complexes plotted in Fig. S5. The excluded solvent volumes were obtained using the same crystal structure as modified in the present work, using probe radius of 1.2 Å and a grid spacing of 0.7 Å.

Complex	Nd**L**	Eu**L**	Gd**L**	Tb**L**	Ho**L**
Pore volumes (Å ^{3})	57.88	57.74	59.28	59.26	13.23
% of cell volume	3.6	3.6	3.7	3.7	0.8

3. Electronic transitions of LnL

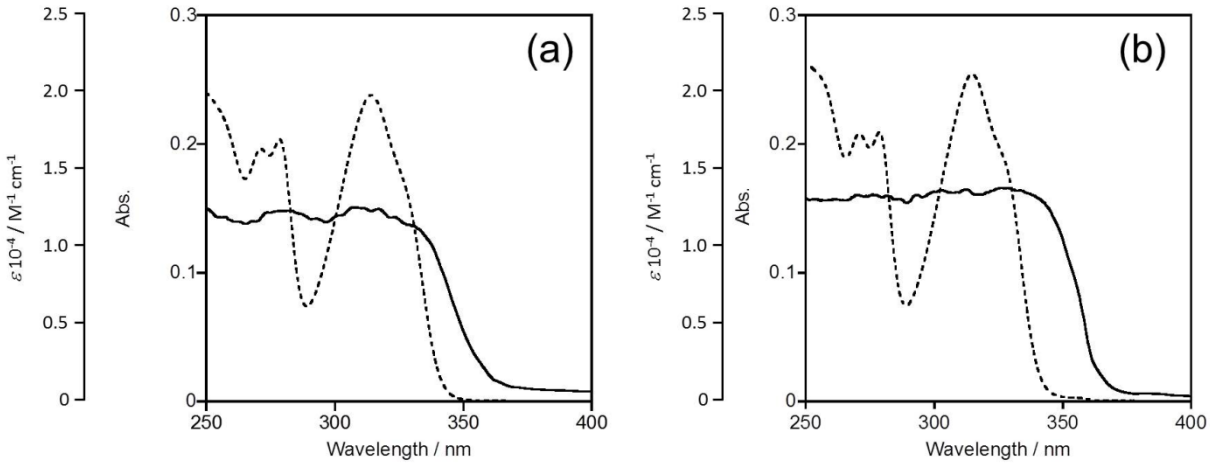

Fig. S6 Electronic absorption spectra of Nd**L** (a) and Ho**L** (b) localized mainly on π-electronic moietis in the solid state (solid line) and in acetonitrile (dotted line).

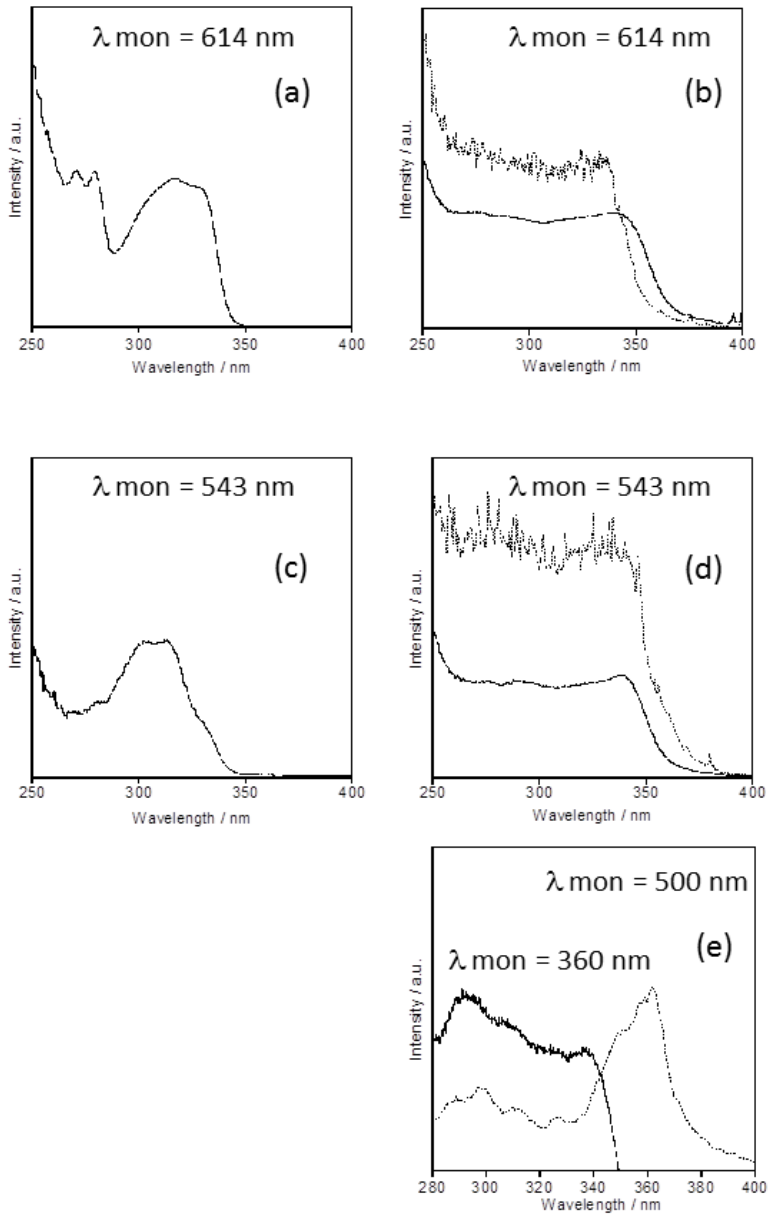

Fig. S7 Excitation spectra of (a) Eu**L** in acetonitrile, (b) Eu**L** at rt (solid line) and 77 K (dotted line) in the solid state, (c) Tb**L** in acetonitrile, (d) Tb**L** at rt and 77 K in the solid state, (e) Gd**L** at rt and 77 K in the solid state.

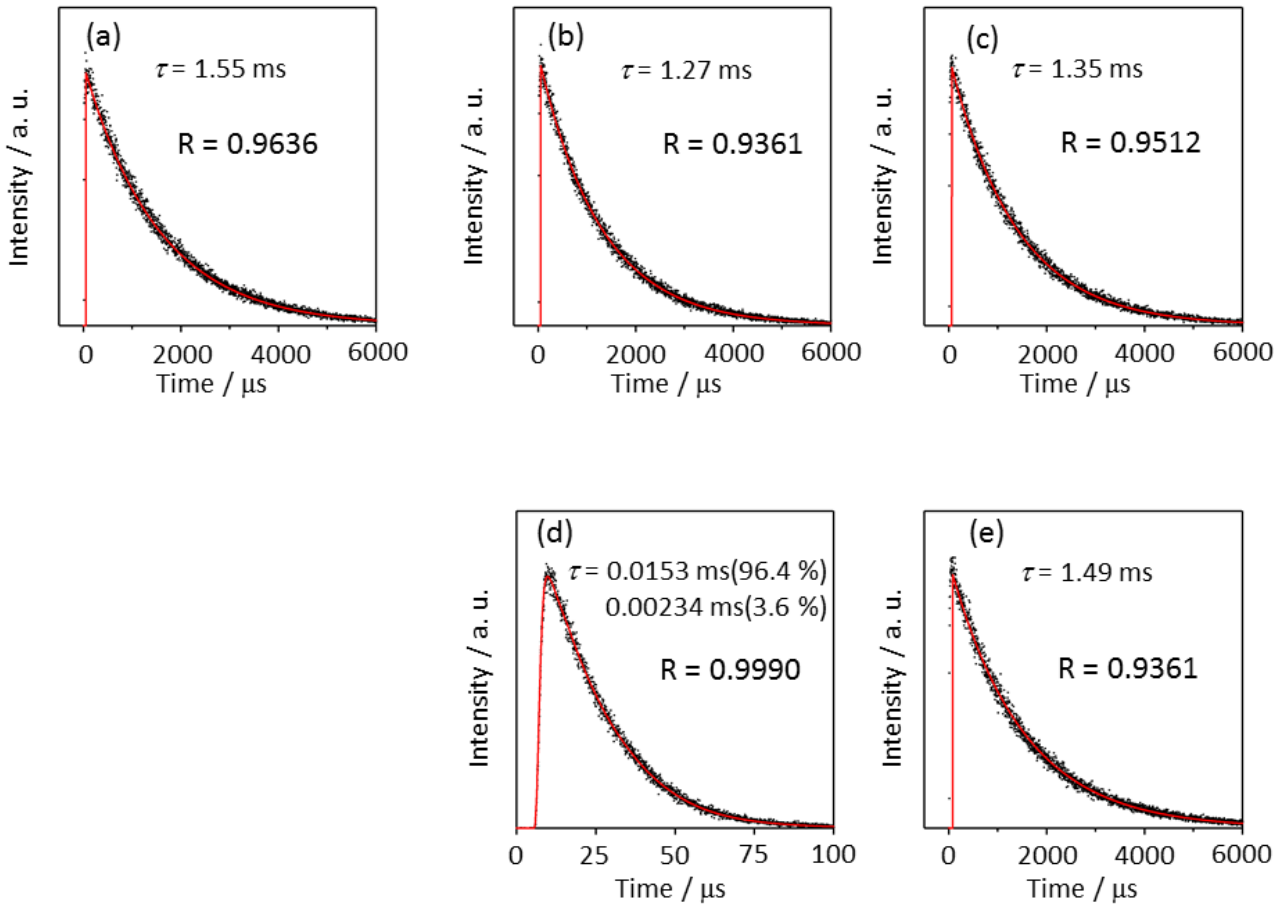

Fig. S8 Decay profiles for the ff emission of Eu**L** and Tb**L** in a) acetonitrile and in b-e) the solid state at various temperatures; (a) Eu**L** in acetonitrile at rt, (b) Eu**L** at rt,(c) Eu**L** at 77 K, (d) Tb**L** at rt and (e) Tb**L** at 77 K. R values for all show presumable values (over 0.9) to discuss them.

5

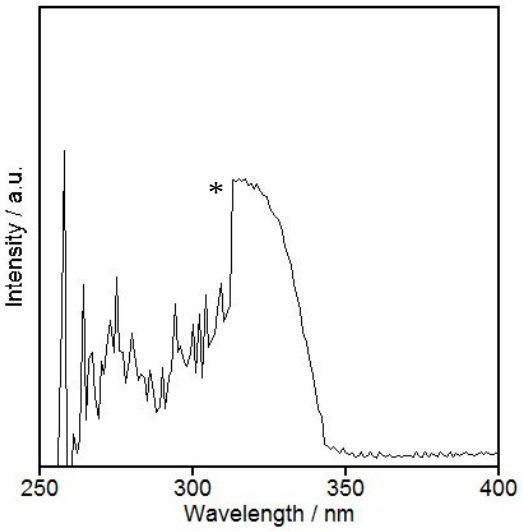

Fig. S9 Excitation spectrum of Nd**L** in acetonitrile monitored at 1055 nm (* due to apparatus).

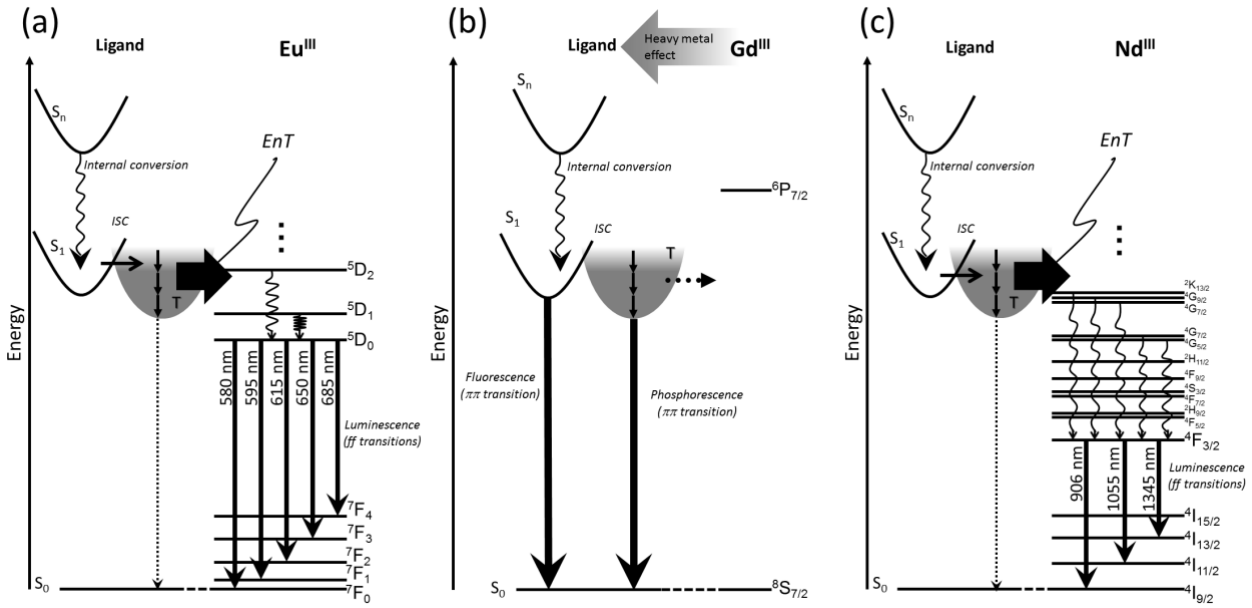

Fig. S10 Schematic representation of plausible energy diagram of the electronic transitions of (a) Eu**L**, (b) Gd**L** and (c) Nd**L**.